04

Influence of RF discharge in H_2-Ne mixture on surface topography and light transmission of sapphire

© A.E. Gorodetsky,[1] V.L. Bukhovets,[1] A.V. Markin,[1] R.Kh. Zalavutdinov,[1] A.P. Zakharov,[1] T.V. Rybkina,[1] S.I. Pozin,[1] V.A. Kabanova,[1] O.Yu. Grafov,[1] E.E. Mukhin,[2] A.G. Razdobarin[2]

[1] Frumkin Institute of Physical Chemistry and Electrochemistry, Russian Academy of Sciences,
119071 Moscow, Russia
[2] Ioffe Institute,
194021 St. Petersburg, Russia
e-mail:valentin_b53@mail.ru

Received February 20, 2025
Revised April 22, 2025
Accepted April 24, 2025

Three effects of cleaning plasma on the surface topography and transmission stability of a sapphire window are investigated. Firstly, the effect on the surface of long-term exposure to a capacitively coupled RF discharge in a 77 % H_2-23 % Ne mixture is considered. Secondly, changes in the structure of sapphire surface layers formed during long-term exposure to the cleaning plasma after removal of thin Al films are analyzed. Thirdly, changes in the structure of sapphire surface layers after triple deposition and subsequent removal of Al films are studied. The demonstrated transmittance stability of r-Al_2O_3 plates allows the use of an r-sapphire window to protect the „first mirror" of the ITER divertor Thomson scattering diagnostic system, as well as in other optical diagnostics in today's fusion research machines and tomorrow's fusion power plants.

Keywords: *R*-sapphire, protective window, AFM surface imaging, Al films, cleaning, ITER.

DOI: 10.61011/TP.2025.11.62231.24-25

Introduction and problem statement

It is planned to use several optical diagnostics to analyze plasma parameters in the International Thermonuclear Experimental Reactor (ITER), in particular, diagnostics of Thomson scattering (DTS) on free electrons [1,2].

In the DTS technique, the scattered laser radiation is collected by an optical system located inside the vacuum volume of the ITER. The most complex component of an intra-vacuum optical light collection system is the so-called plasma-facing mirror, which is supposed to be made of molybdenum [3]. Next, the scattered light will be transmitted to polychromators using a mirror-lens system to analyze the intensity (electron concentrations in plasma, n_e) and the width of the scattering spectrum (electron temperatures, T_e) [4]. In general, it is planned to install more than 30 „first" metal mirrors in ITER for plasma diagnostics using various optical methods [5].

The „first" mirrors will be subjected to significant thermal loads and the effects of neutral atom fluxes from plasma containing material elements of the inner lining of the tokamak chamber. Carbon, oxygen, beryllium, and tungsten were considered typical deposited impurities on the „first" mirrors [3,5]. Based on experiments on operating tokamaks (for example, [6,7]) in 2024, it was decided to abandon beryllium on the inner wall of the main chamber of the ITER and replace it with a tungsten coated with a layer of boron. In this regard, the appearance of boron-based compounds on the first mirrors is quite possible.

To preserve the optical properties of the first mirrors, it is necessary to develop a protection system against the adverse effects of plasma and radiation, as well as from contamination by erosion products of the first wall. Film deposits containing boron condensed on the mirror will lead to a decrease in its reflectivity. It was proposed in Ref. [8–10] to use radio frequency (RF) discharge plasma for cleaning the first mirrors. The possibility of protecting the „first" DTS mirror with a window made of a sapphire plate (single crystal Al_2O_3) with a thickness of $1-2$ mm was considered in Ref. [1,2]. Currently, it has been decided to manufacture the protective curtain of the „first" DTS mirror from sapphire. In this case, it is proposed to equip both the first mirror and its sapphire curtain/window with a plasma cleaning system, the design of which is under development. The curtain is supposed to be cleaned in the open state, in which it is located opposite a special RF electrode. When placing RF cells in the main chamber, the direction of the strong magnetic field should be taken into account in order to minimize its effect on the parameters of the cleaning RF discharge.

Sapphire (α-Al_2O_3) is transparent in the wavelength range of $300-1100$ nm for most optical diagnostics methods, chemically inert, durable and heat-resistant dielectric with high thermal conductivity and high dielectric constant [11,12]. Depending on the optical polishing technique, the thickness of the primary disturbed layer can vary from 0.1 to 2 μm [13].

If the crystal plane of a sapphire lattice with Miller indices (0001) is parallel to the surface, then such plates

are indicated in the text below as c-C. In the case of the plane $(1\bar{1}02)$ parallel to the plate surface is denoted as r-C. The angle between the planes $(1\bar{1}02)$ and (0001) in the sapphire lattice is 57.6°.

Taking into account the experiments on tokamaks [14,15], a mixture of neon and hydrogen was chosen as the working gas for the cleaning RF discharge. Aluminum was chosen as the deposited metal, used as a model, polluting material in experiments with the „first" mirrors [16] instead of the boron expected in ITER. It is stated in Ref. [16] that when aluminum and boron are deposited on the surface of metals, aluminides and borides are formed that retain hydrogen, and the patterns of hydrogen capture and retention in these compounds are similar.

Boron, like aluminum, forms a solid oxide in Al_2O_3 Unlike Al_2O_3 boron oxide has a low melting point, but both oxides, covering the surfaces of solid Al and B, slow down oxidation. Aluminum, like boron, does not restore sapphire at low temperatures. Possible reactions of boron with sapphire during plasma purification from boron contaminants require a separate analysis.

The authors like in Ref. [17] believe that during cleaning, due to the uneven removal of impurities from the surface of r-C, it will take some time to apply plasma directly to the surface layer of the sapphire window. Therefore, for effective and reliable use of an RF discharge, it is necessary to investigate the change in the structure and topography of the sapphire surface cleaned as a result of prolonged plasma exposure and the associated change in light transmission r-C.

The purpose of this study is to analyze three possible effects of the discharge on the sapphire window. First, consider the effect of prolonged exposure to a cleaning discharge of 77%, $H_2-23\%$, Ne on the structure and composition of the surface layer of r-C and on the optical stability of sapphire in terms of its light transmission. Secondly, study the changes in the surface layers of sapphire formed by prolonged exposure to RF discharge after application and purification from the Al film. Thirdly, consider the changes in the surface layers of sapphire after three-fold precipitation of Al and its subsequent removal by RF plasma discharge.

The formulation of this problem is caused by the proposed use of sapphire as protective and vacuum windows in ITER, as well as the widespread use of sapphire (r-C) in microelectronics as substrates in silicon structures on sapphire [18].

The light transmission coefficient (TC) like in Ref. [17] in the wavelength range of DTS (400−1100 nm) was chosen as the criterion for the optical stability of the window material.

1. Experimental procedure

Five square sapphire plates $10 \times 10 \times 1$ mm, optically polished on both sides, were provided by „Fluorite" LLC, St. Petersburg. Before the experiments, the plates were cleaned in hexane.

In the proposed scheme of plasma action on sapphire, a DC discharge was used in a quartz tube with an inner diameter of 19 mm between a hollow cathode and a grounded anode. An RF capacitive discharge was formed between a high-voltage electrode with an area of 2.27 cm^2 connected to an RF generator of 13.56 MHz and a grounded electrode with an area of 10 cm^2. The RF discharge electrodes were positioned opposite each other in the center of the positive column. An RF generator (with a power of 50 W) created an offset of −300 V on the surface of a plate of r-C. During the experiments, the sample temperature did not exceed 100 °C [8,10,17]. The pressure in the RF discharge was maintained at 15 Pa at a flow rate of a mixture of hydrogen and neon 13 sccm. The flow of Ne (3 sccm) was 23 % of the total flow of a mixture of H_2 and Ne (hereinafter H_2-Ne). The cleaning discharge parameters used in the laboratory installation can be scaled when they are adapted to the ITER conditions.

The determination of the r-C spray rate was carried out by weighing the samples on a balance (with an accuracy of 0.5 μg) before and after plasma exposure. The elemental composition of the samples up to depth 1 μm was determined by X-ray energy dispersion spectroscopy. The samples were analyzed by X-ray photoelectron spectroscopy (XPS) using an ESCA+ spectrometer (OMICRON, Germany) in monochromatic radiation Al K_α 1486.6 eV. The transmission energy of the analyzer was set to 120 eV when measuring the survey spectrum and 20 eV when measuring the lines of individual elements. The effect of charging the sample was taken into account by shifting the analyzer's energy scale so that the peak of C 1s hydrocarbon pollutants (adsorbed impurities from the atmosphere during sample transfer) was located at 285.0 eV.

The relief and surface roughness of r-C were analyzed using an EnvirScope atomic force microscope (hereinafter AFM) in semi-contact mode with a silicon cantilever with a radius of 10 nm manufactured by TipsNano (Zelenograd). The morphology of the surface was monitored using an optical microscope (OM).

The structure of r-C was studied by X-ray diffraction for reflection (scheme $\theta-2\theta$) in Si radiation K_α when the plate rotates around an axis normal to the surface at the speed of 0.7 rps [17].

The optical properties of r-C were studied on a stand assembled from fiber-optic components manufactured by AVANTES (www.avantes.com) using a halogen lamp as a light source. The error of recording the transmission in the range of 500−800 nm was 1 %. The details of the measurements are described in our previous paper [17]. A Shimadzu UV-3101PC spectrophotometer (Japan) was used for measurements in the range of 190−1200 nm. The width of the light beam in the plane of the measured sample was set to about 1 mm. The beam height was determined by a diaphragm with a circular hole with a diameter of 7 mm. The sample was fixed to the diaphragm with adhesive tape.

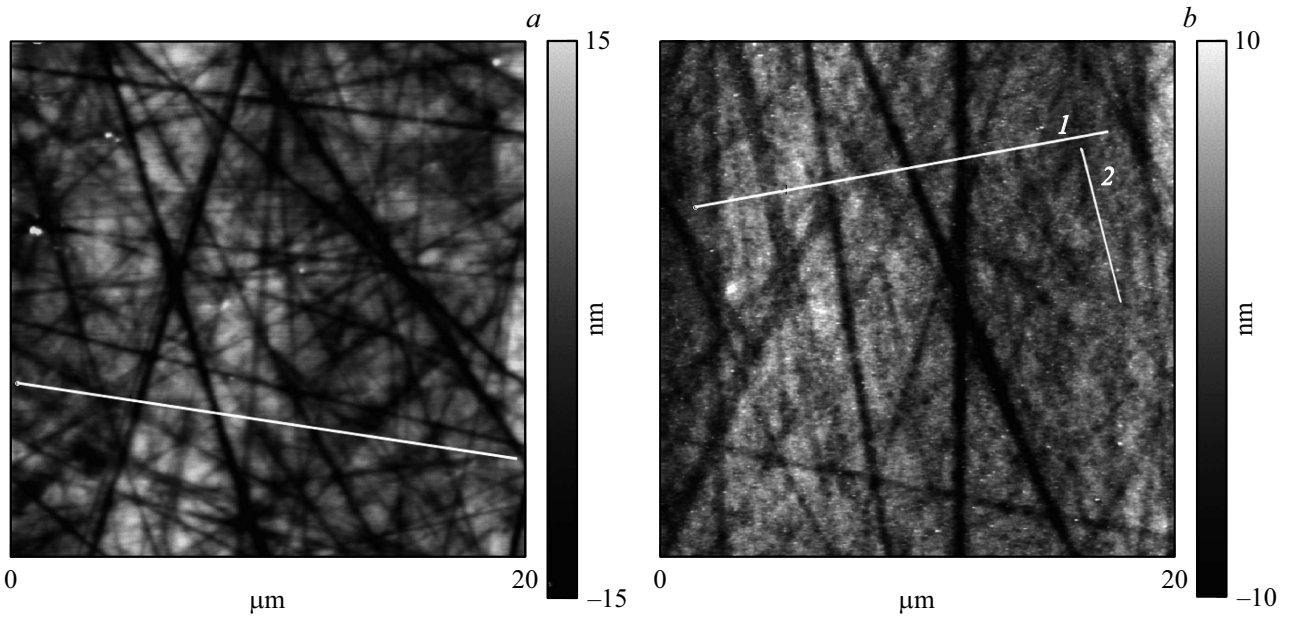

Figure 1. AFM image of the surface topography r-C (area $20 \times 20\,\mu$m) after mechanical polishing (a) and after exposure to RF discharge in a mixture of $H_2-23\,\%$ Ne for 12 h (b).

The error of recording the transmission over the entire range was less than 1 %.

The Al film was applied to the surface of the plate r-C by thermal evaporation of aluminum (purity 99.99 mass%) from a tungsten spiral at a pressure of $(4-8)\cdot 10^{-4}$ Pa. The deposition rate varied in the range of 3–10 nm/s.

2. Experimental results and their discussion

According to X-ray diffraction data, the r plane with Miller indices $(1\bar{1}02)$ was parallel to the surface of the plates. The distance between r-planes d, calculated from the reflex $(1\bar{1}02)$ at an angle of $2\theta = 25.49°$, turned out to be equal to (0.3491 ± 0.0001) nm [19] and close to the standard value for a single crystal of leucosapher [12]. Annealing in air at 700 °C did not lead to a change in the plate structure analyzed by X-ray diffraction.

According to energy dispersion spectroscopy, traces of iridium were present in the sapphire samples. The elemental composition of the plates, determined using the MULTIFILM program, turned out to be stoichiometric: 40 at.% Al and 60 at.% O.

With a normal drop in the luminous flux, the TC of light in the wavelength range 400–1200 nm in the plates r-C was 85–86 % and was close to the tabular values.

The addition of neon to the hydrogen plasma of an RF discharge increased the steady-state mass sputtering rate r-From (3.6 ± 0.2) to $(9.0 \pm 0.2)\,\mu$g/(cm$^2\cdot$ h). At a density of r-C ρ equal to 3.98 g/cm^3, the linear spray velocities were (8.9 ± 0.1) nm/h and (22.5 ± 0.1) nm/h, respectively. The plasma exposure was not accompanied by the introduction of impurities into the surface layer analyzed by energy dispersion spectroscopy.

The initial surface of r looked quite smooth. The main visible defects are scratches or grooves (about 1 μm wide) that occur during polishing. After 12 h exposure in plasma and removal of 270 nm layer of material, polishing grooves remained. They filled the entire surface of the plate evenly.

According to the AFM data, the width of the polishing grooves on the initial surface varied from 0.1 to 0.5 μm, and the depth varied from 1 to 8–12 nm (Fig. 1, a and 2, a). As a rule, the depth of the pits at the intersection points of the two grooves is greater than the depth of each groove. In the cross-section (Fig. 2, a) along the white line (Fig. 1, a), protrusions or dumps up to 10 nm high are visible on the sides of the grooves. The RMS roughness R_q was 5.4 nm.

After exposure in the discharge, the polishing grooves are up to 1 μm wide and up to 8 nm deep (Fig. 1, b, line *1* and Fig. 2, b) remained. The dumps along the scratches began to look less contrasting. The number of grooves in the length of 16 μm decreased from 10 to 8. Bridges up to 1 μm wide appeared on shallow grooves with a depth of less than 8 nm. During the spraying process, short gaps up to 10 μm appeared in the extended grooves (Fig. 1, b). After irradiation, the roughness decreased to $R_q = 3.4$ nm. In the presented section (Fig. 2, b), relatively deep depressions separated from each other by 1 μm, — this is the intersection of the grooves with the cantilever. More frequent relief differences between the grooves are elements of a new structure that appeared as a result of exposure to radio frequency discharge.

The resulting thin submicron relief (Fig. 3, a) can be characterized by an alternation of light protrusions and dark depressions with a diameter of 0.1–0.3 μm in height and

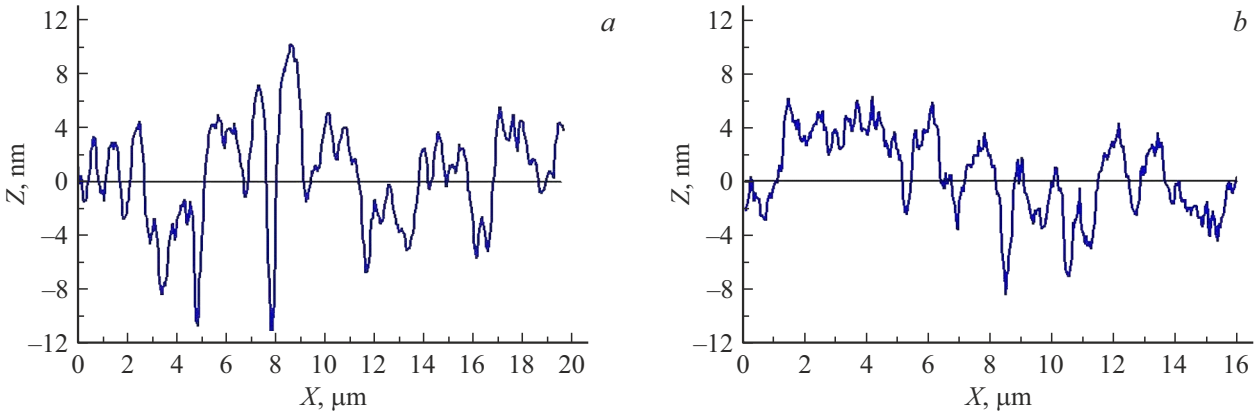

Figure 2. Relief differences along the lines shown in Fig. 1, *a* and *b* (line *1*): after mechanical polishing (*a*); after exposure to discharge (*b*).

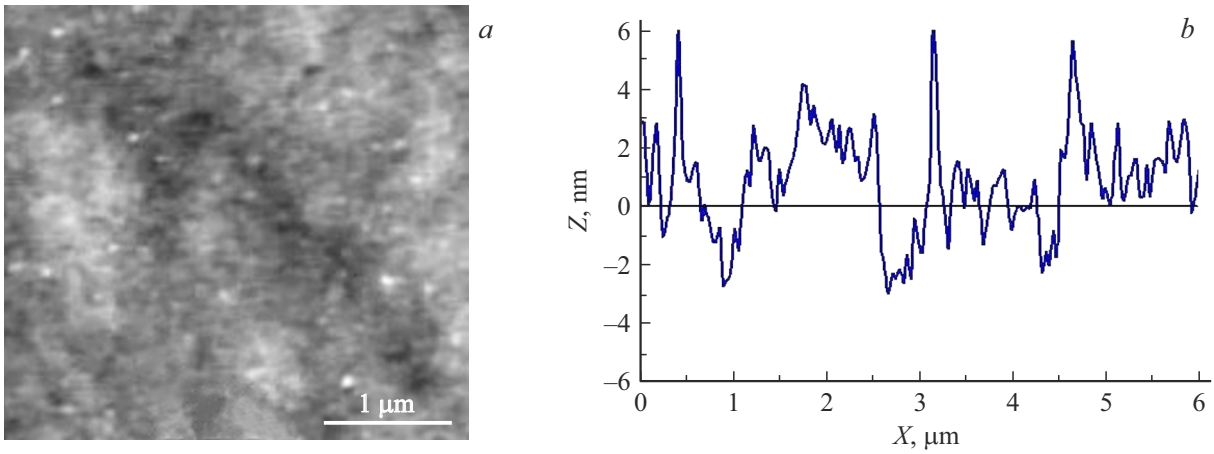

Figure 3. Topographic image of the surface area between the grooves (*a*) and the relief differences along the line *2* in Fig. 1, *b* (*b*).

depth of 4–6 nm with a surface density of $6 \cdot 10^{12}$ cm^{-2}. Typical shapes and sizes of protrusions and depressions (Fig. 3, *b*) are shown in the cross section plotted along the line *2* is 6 μm long (Fig. 1, *b*). The ratio h/r of the height of the projections (h) to their lateral size (r) is usually $\sim 0.01-0.02$. The protrusions are shaped like a segment of a ball with a radius of $R \approx r/2(r/h) \approx 10\,\mu$m, much larger than h. The protrusions appear to be rather flat islands with an angle of inclination of the side surface to the base about 1°. The distance between the projections was 0.2–0.3 μm. The protrusions alternating with depressions represent a new element of the topographic relief formed by prolonged irradiation (Fig. 3, *b*). The roughness in such areas decreased to $R_q = 1-2$ nm.

These facts indicate a gradual removal of grooves. Simultaneously with the removal of polishing grooves, a new structure is formed in local areas of the surface from small protrusions (nanoislands) and depressions (nanocavity, nanoholes) with a total height difference not exceeding 8–10 nm. These areas have a reduced roughness ($R_q < 2$ nm). After 12 h of RF exposure, the light transmission coefficients in the wavelength range of 400–1000 nm, measured at the Avantes stand, remained virtually unchanged from the initial baseline values.

Due to the possibility of re-deposition of the spray products of the first wall onto the cleaned surface of the protective window, in the second series of experiments, after 12 hours of exposure in an RF discharge, an Al film with a thickness of 80 nm and a weight of 21.6 μg/cm^2 was deposited on the plate *r*-C (Fig. 4, *a*). The morphology pattern of the solid Al film on the surface completely copied the relief of the sapphire substrate (Fig. 4, *a*). The light efficiency of the Al condensed film plate did not exceed 1 %. Next, the the Al film was removed from sapphire. The time to remove the aluminum film until the transmission was fully restored was about 2 h. According to OM (Fig. 4, *b*), the Al film was removed mainly by local peeling of areas with an area of 1–10 μm^2. Dark areas in Fig. 4, *b* are places with an open sapphire surface, grayish areas are peeled off but not removed areas of the film, light green areas are areas of the Al film firmly bonded to the substrate. During further exposure in the RF discharge, the detached film sections were carried away by the gas stream. The remaining Al islands were removed by physical spraying together with

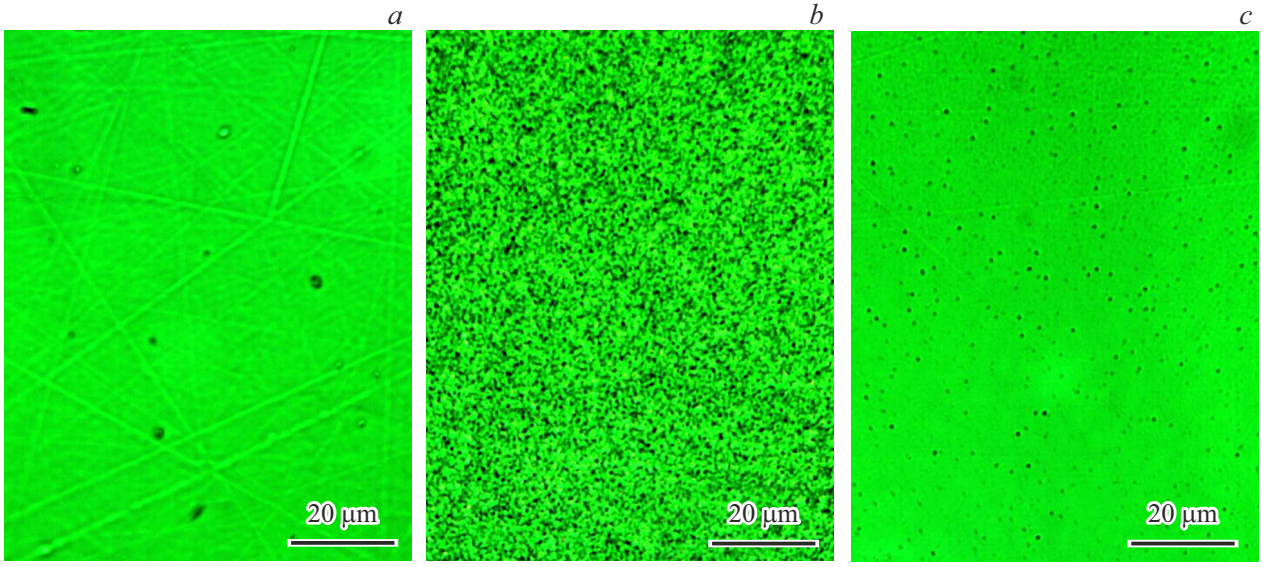

Figure 4. Morphology of the initial Al film in ohms (a), after exposure in an RF discharge in a mixture of H_2-Ne for 20 min (b) and a purified sapphire surface (c).

spraying of r-C substrate. AFM surface analysis showed that the black dots that appeared on the cleaned surface of the sapphire (Fig. 4, c) correspond to pits.

After total cleaning during 2.3 h and removal of metallic Al, the roughness increased from the initial $R_q = 3.4-3.6$ nm to $R_q = 4.9-5.0$ nm. The topographic pattern of the surface has undergone significant changes (Fig. 5). Polishing grooves up to 10 nm deep were almost completely etched. The newly formed surface structure resembled a cellular structure of pits with a depth of 5–10 nm in relation to the surrounding protrusions with a height of 3–5 nm. The distance between the pits was 0.4–0.6 μm. The width of the protrusions surrounding the pits was 0.2–0.3 μm.

If, before cleaning, areas of protrusions and depressions were formed in the areas between the grooves with distances between the protrusions up to 0.3 μm (Fig. 6, a), then after cleaning from the Al film, the distance between the pits increased to 0.6–0.8 μm (fig. 6, b). The angles of inclination of the lateral surfaces of the pits relative to the average flat bottom did not exceed 1°.

As a result of the purification in the RF discharge, the light transmission, which was reduced due to the deposition of the Al film, was completely restored to its original value (Fig. 7).

For clarity, the light transmission spectrum is divided into two length ranges. It can be seen that in the range of 300–700 nm (Fig. 7, a), the TC values of the original plate (spectrum *1*) are lower than the TC of the sapphire plate with removed aluminum film (spectrum *2*). Defects in the surface layer of sapphire that occur during mechanooptical polishing probably lead to additional transmission losses in the range of 300–700 nm. The spectrum it2 coincides with the calculated spectrum it3 in this wavelength range. The calculations were performed in the Optical program [20]. Refractive index values in the range of 200–1200 nm are taken from Ref. [21,22].

In the wavelength range of 200–350 nm, the difference between the experimental and calculated spectra *3* is probably caused by the absorption of light by various structural disturbances. In length intervals of 700–800 nm (Fig. 7, a) and 900–1200 nm (Fig. 7, b) the light transmission of the initial the plates and plates peeled from the Al film practically do not differ and coincide with the calculated TC with an accuracy better than 1 %. The increased TC fluctuations in the range of 800–900 nm are caused by the use of a lead sulfide-based PbS detector in this range. Switching to a photoelectric multiplier was set at 800 nm.

According to the XPS data, only aluminum, oxygen, and carbon from surface pollutants are represented in the overview spectrum of the cleaned plate (Fig. 8, a). The peak maximum of Al $2p$, marked by arrow Al^{3+} in Fig. 8, b, corresponds to the binding energy of 74.6 eV. Analysis of the position and width of this peak in the UNIFIT program shows that aluminum is found only in the oxide Al_2O_3. The position of the peak of the photoelectrons of the reduced metal with a binding energy of 72.6 eV is indicated by the arrow Al^0 in Fig. 8, b. The absence of a signal from photoelectrons with a binding energy of 72.6 eV (Fig. 8, b) indicates that there is no metallic Al on the surface of the purified sapphire. It is possible that aluminum was reduced from oxide in a thin surface layer during sputtering in an RF discharge, but upon contact of the sample with air, the metal was oxidized to Al_2O_3.

In connection with the proposed periodic cleaning of the protective window from deposited films, in the third series of experiments, a film of Al with a thickness of 30–40 nm

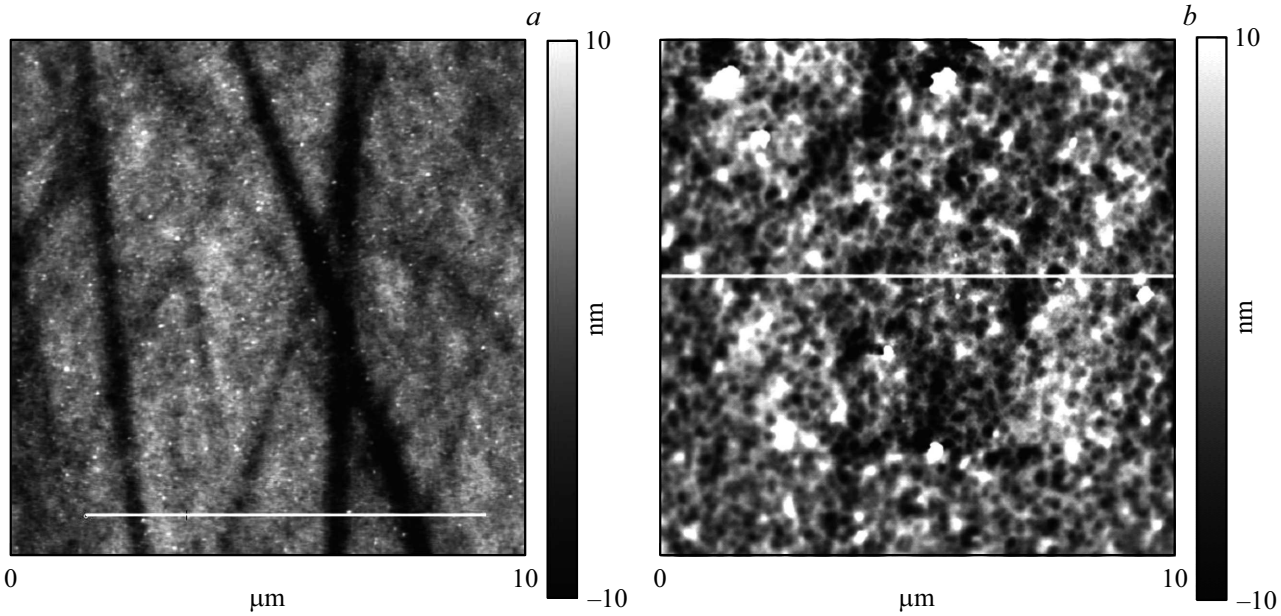

Figure 5. AFM image of the topography of surface of *r*-C after exposure in RF discharge for 12 h (*a*) and after application and subsequent cleaning from 80 nm thick Al film for 2.3 h (*b*).

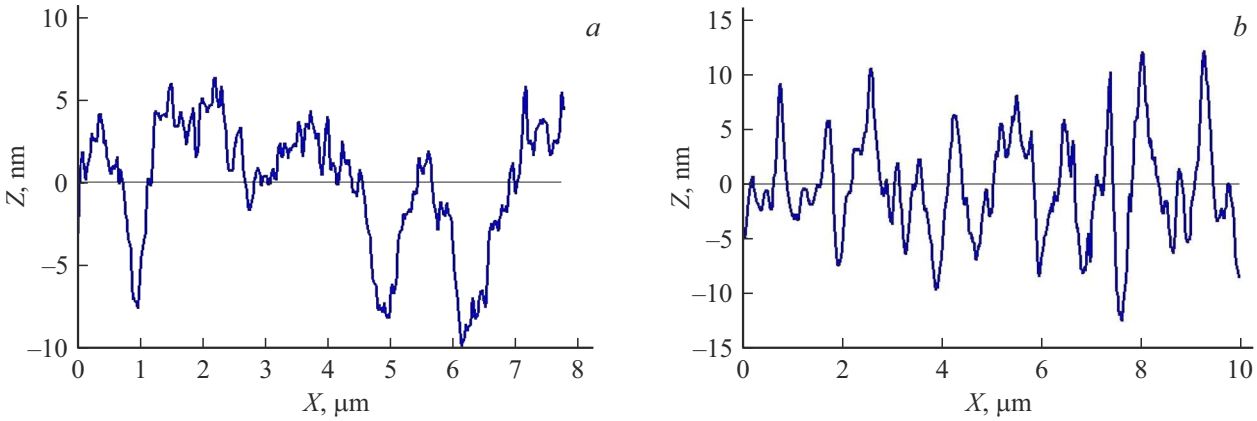

Figure 6. Relief differences along the white lines in Fig. 5, *a* (*a*) and *b* (*b*).

was deposited three times on the initial, mechanically polished surface *r*-C. After each Al deposition, the plate was cleaned in an RF discharge of H_2-Ne for 1 h. In this experiment, traces of polishing grooves remained (Fig. 9), since the total exposure time of the cleaned surface *r*-C did not exceed three hours (the thickness of the removed sapphire layer is < 40 nm).

As in the case of purification from Al after prolonged exposure in the second series of experiments (Fig. 5, *b*), the surface of *r*-C presented a cellular structure (Fig. 9, *a*).

The application and subsequent removal of the Al film resulted in the formation of a new topographic surface pattern. Enlarged pits (700–1500 nm) surrounded by relatively thin sides (Fig. 10, *b, c*) appeared instead of a relief of weakly pronounced protrusions and depressions (Fig. 10, *a*) with a size of 200 nm at the base.

r-C plate did not transmit light after each cycle of deposition of the Al film. As a result of the subsequent 40-minute exposure in the RF discharge, the sapphire's TC was restored to its original values. Fig. 11 shows the light transmission after the final, third cleaning from the Al film. It can be seen that the light transmission values in the range of 900–1200 nm of the initial plate 1 and the cleaned plate *2* differ by less than 1 % (Fig. 11).

As a result of mechanical polishing, the surface of the initial plates was covered with polishing grooves with dumps (sides) along the grooves and had a roughness of $R_q = 5.4$ nm. After prolonged exposure in the RF discharge, the roughness decreased to $R_q = 3.4$ nm, mainly due to spraying of the sides. The predominant spraying of the sides is probably due to their defects. At the same time, areas of a new structure with $R_q = 1-2$ nm appeared between

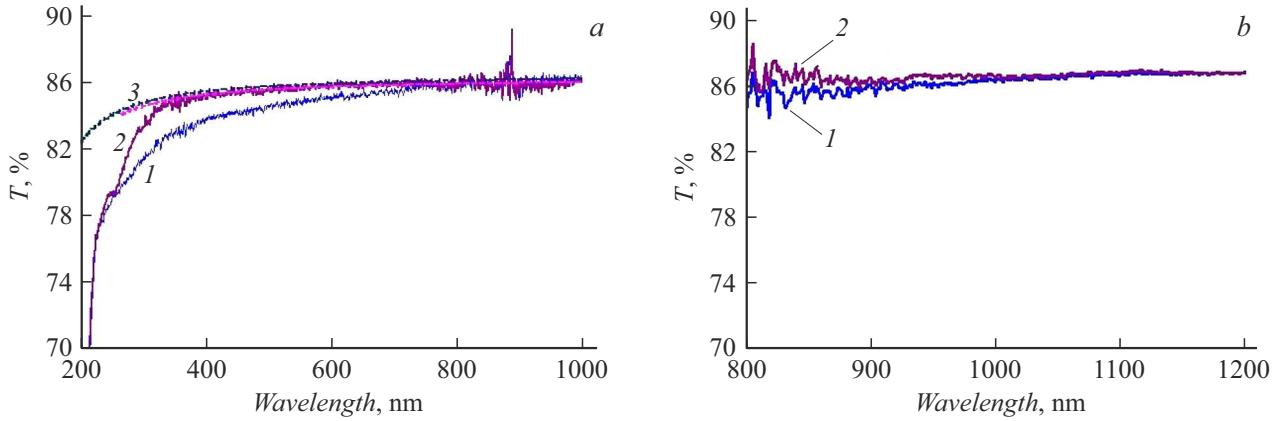

Figure 7. Light transmittance (T) of plates of r-C before (1) and after exposure in RF discharge in a mixture of $H_2-23\,\%$ Ne for 12 h followed by application of an Al film with a thickness of 80 nm and cleaning in discharge for 2.3 h (2), calculated TC of plates of sapphire (3); wavelength range of 200–1000 nm (a) and 800–1200 nm (b).

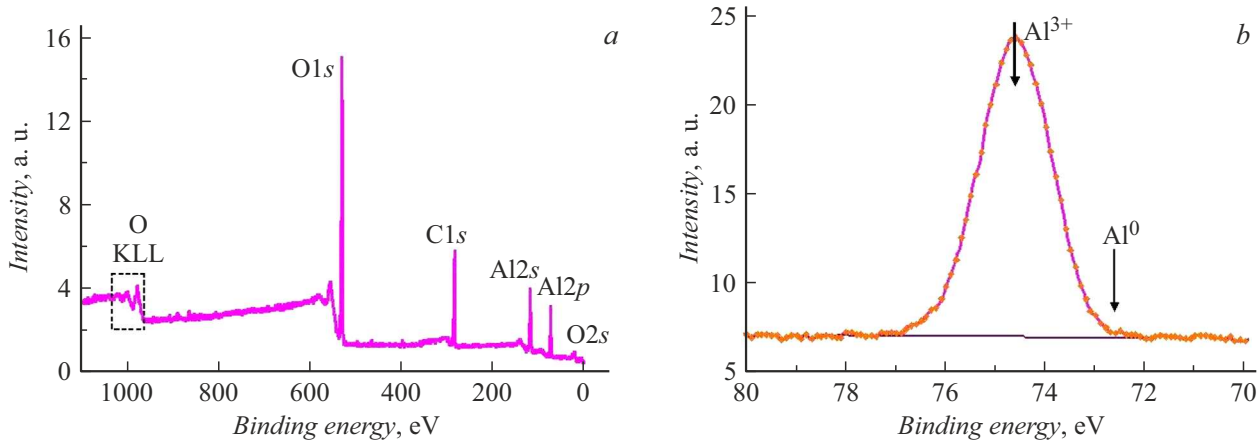

Figure 8. RF spectra of the sapphire surface after exposure to RF discharge in a mixture of $H_2-23\,\%$ Ne for 12 h, followed by the application of an Al film with a thickness of 80 nm and cleaning in discharge for 2.3 h; panoramic spectrum (a) and spectrum of Al 2p (b).

the grooves. Unlike the spraying of the sides created by mechanical polishing, in these areas the spray rate in the local depressions is higher than on the neighboring projections. However, starting with some fluences, the deepening of the depressions may stop due to ion-stimulated movement of the Al_xO_y complexes in the direction from the protrusions to the depressions [23–25]. Local areas with low roughness (Fig. 3, a) and formed protrusions/depressions (Fig. 3, b and 10, a) may be emerging areas of stationary the structure that occurs during prolonged exposure of a sapphire plate in an RF discharge.

In the described experiments the energy of atomic and molecular charged particles of hydrogen and nitrogen colliding with the target varied in the range from 0 to 300 eV [{]8,10}. According to calculations using the SRIM program, the path length did not exceed 5 nm even for the lightest ions H^+ with a maximum energy of 300 eV [26]. In experiments, the path length of the embedded ions was much less than the thickness of the sputtered layer (270 nm).

In the stationary state, due to the predominant oxygen sputtering, the increased content of the metallic oxide component in the surface layer does not depend on the exposure time in the discharge in the absence of oxygen diffusion from the target volume. This means that partial or complete reduction of the oxide must occur in the surface layer. At the same time, the spray flow must remain constant and stoichiometric.

Thermodynamic estimates of the reduction of some oxides by atomic hydrogen are given in Ref. [27]. The evaluation of the change in Gibbs free energy (ΔG) during the reaction of sapphire with atomic hydrogen, carried out according to the method described in [28], shows that the reduction of Al_2O_3 is quite probable.

If we assume that the chemical potential of two hydrogen atoms adsorbed on the surface or embedded in the sapphire lattice is 438 kJ/mol H_2 higher than the molecule H_2, then reactions of complete reduction of sapphire with the formation of metallic aluminum are possible (1) or partial reduction to form hydroxide (2). The free energies of the

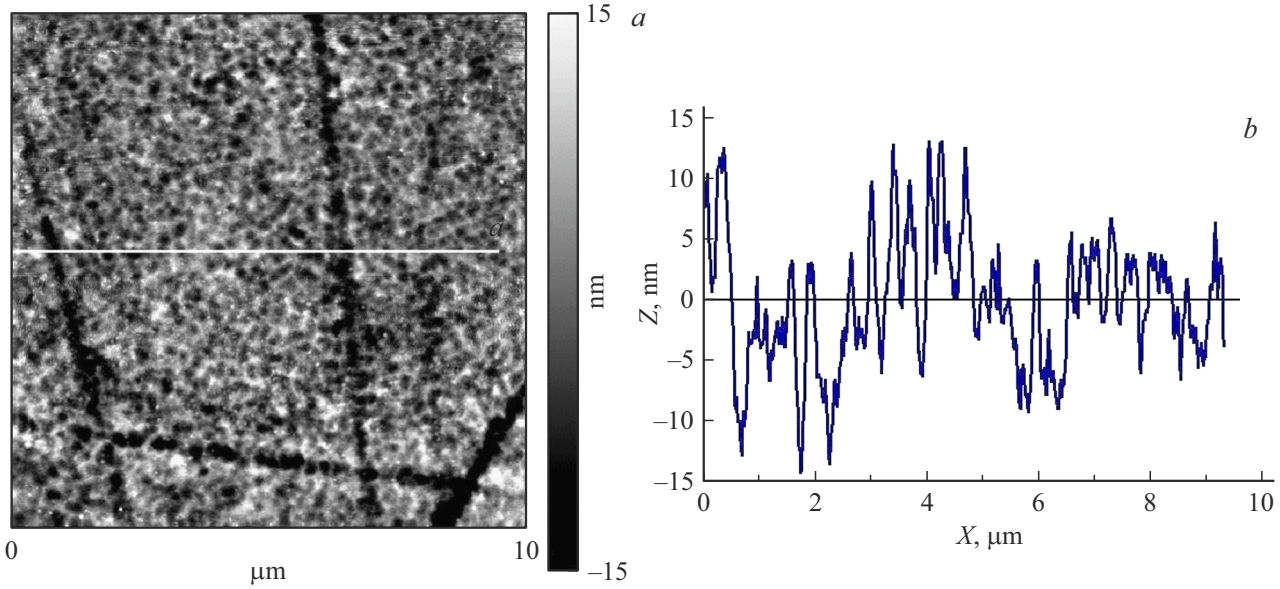

Figure 9. AFM image of the topography of surface of *r*-C after triple application of Al film with the thickness of 30–40 nm and triple cleaning in RF plasma, $R_q = 5.6$ nm (*a*); relief differences along the line shown in the AFM image (*b*).

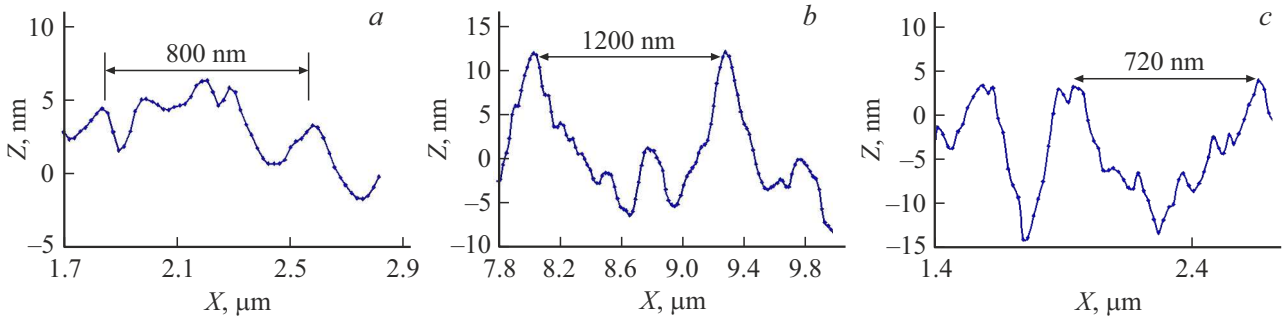

Figure 10. The most characteristic relief changes in magnified scale along the axis *X*: after prolonged exposure in RF discharge, the line *2* in Fig. 1 (*a*), after a single cleaning, Fig. 5, *b* (*b*) and after a triple cleaning, *c*).

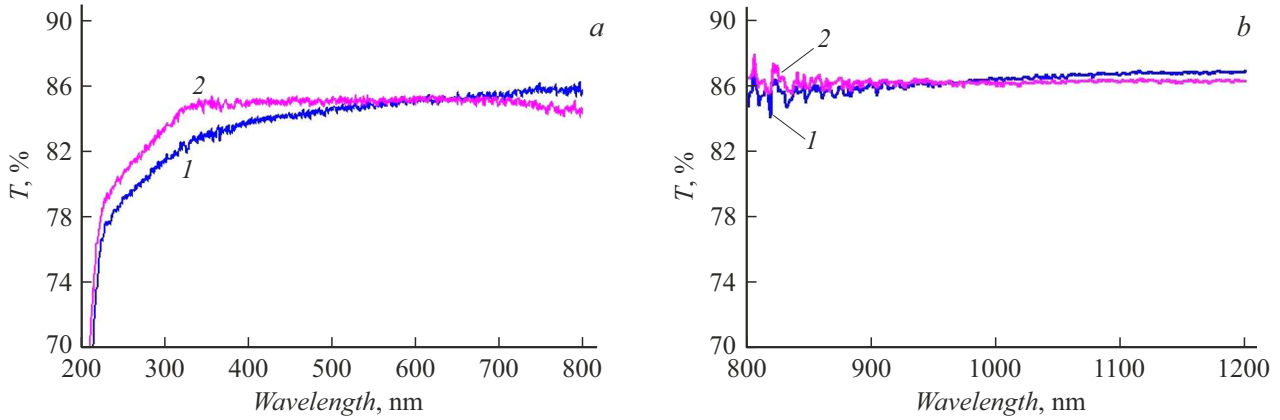

Figure 11. Light transmission coefficients of the initial plate *r*-C (*1*) and the plate after triple deposition of an Al film with a thickness of 30–40 nm and triple cleaning in plasma in a mixture of H_2–Ne (*2*). Total plasma exposure time 2.3 h; wavelength range 200–800 nm (*a*) and 800–1200 nm (*b*).

reaction components are taken from Ref. [28]:

$$4H + 2/3\,Al_2O_3 = 4/3\,Al + 2\,H_2O\,(g), \qquad (1)$$

$$\Delta G_{300\,K}\,(kJ/(4\,mol.H)) = \Delta G\,(init.) - \Delta G\,(prod.) = -216.33\,kJ/(4\,mol.\,H).$$

$$3H + Al_2O_3 = Al + AlOOH\,(sol.) + H_2O\,(g), \qquad (2)$$
$$\Delta G_{300\,K}\left(kJ/(3\,mol.\,H)\right) = -171.84\,kJ/(3\,mol.\,H).$$

Reaction (2) is preferable in terms of 1 mol of atomic hydrogen.

The source of the atomized target atoms are the two or three uppermost atomic layers [29]. It is in these layers that stoichiometry violations should be expected. However, the fluxes of residual oxygen atoms and molecules $\left(\sim 10^{14}\,part/(cm^2 \cdot s)\right)$ and the contribution of neon ions to the total sputtering coefficient can offset the effect of sapphire reduction. There were no direct indications of reduction of metallic aluminum in the described experiments.

An unsuccessful attempt to detect the reduction of Al_2O_3 by irradiation with low-energy ions D^+ and He^+ was made in Ref. [30]. At the same time, the predominant nitrogen sputtering in AlN plates was proved. The authors of Ref. [30] believe that due to the lack of selective oxygen sputtering, the use of sapphire windows is promising in large plasma installations in thermonuclear experiments.

The removal of the Al film in the second series of experiments was carried out both by exfoliating local areas of the film in the first 10–20 min exposure in RF discharge, and by physical spraying at the final stages of cleaning. The areas of the sapphire surface that were freed from the Al film by peeling began to spray earlier than the areas still covered with the Al film.

In the areas free of Al, subsequent exposure in an RF discharge for 1 h was accompanied by the removal of a sapphire layer with a thickness of 20–30 nm. The noted increase in surface roughness from the initial $R_q = 3.4$–3.6 nm to $R_q = 4.9$–5.0 nm is caused by uneven removal of the Al film and, as a result, the formation of at least a two-level cleaned surface r-C.

The reduced light transmission ($< 1\,\%$) after deposition of the Al film on the surface of r-C was completely restored to its original value as a result of subsequent purification in an RF discharge.

The triple deposition of an aluminum film with a thickness of 50 nm onto the initial mechanically polished surface and triple cleaning in an RF discharge for 1 h in each cycle was accompanied by the removal of a layer of sapphire with a thickness of 10–15nm and the development of a cellular surface structure against the background of primary grooves left from mechanical polishing.

One of the reasons for the appearance of the cellular structure of the target is the direct process of erosion of the aluminum film with predominant peeling and removal of local areas of size 1–$3\,\mu$m (Fig. 4, *b*). In the surface areas of r-C that appeared free of Al, depressions (pits) surrounded by areas covered with the remaining aluminum film formed as a result of spraying. The removal of aluminum by physical spraying from the remaining areas occurred with a delay relative to the exfoliated areas. The removal of aluminum adsorbed at the surface stages of r-C is most difficult. As a result, the pits are surrounded by stepped sides. The authors observed a similar cellular structure of the surface when cleaning glassy quartz KU-1 from an Al film in an RF discharge of a mixture of H_2–10 % N_2 [31].

After each cleaning cycle, the light transmission coefficient returned to the initial values. The final TC after three times cleaning turned out to be 1 % higher than the initial values in the entire wavelength range.

The restoration of light transmission after purification is associated with the effect of an RF discharge only on the surface layers of the target with a thickness of no more than 30–50 nm. At temperatures not exceeding 100 °C, the defect formation process does not extend into the target volume.

The range of light wavelengths of 800–1100 nm is supposed to be used to determine the temperature and density of plasma in the ITER divertor using DTS. However, the possibility of combining DTS with the diagnosis of laser-induced fluorescence of neutral and singly ionized helium in the wavelength range of 380–710 nm is being considered. The experiments have shown that in the indicated wavelength ranges, plasma purification does not impair the light transmission of sapphire.

The stability of light transmission of plates of r-Al_2O_3 demonstrated in the study after exposure to RF discharge in a mixture of 77 % H_2–23 % Ne in the considered wavelength ranges allows considering the considered metal precipitation purification technique promising for use in restoring the light transmission of sapphire windows in optical diagnostics of the ITER tokamak under construction.

The use of a sapphire protective window in front of the „first“ mirror in a number of optical diagnostics of ITER raises some objections due to the damage of sapphire by neutrons and a decrease in TC in the range of 200–400 nm. The use of a protective window may be useful on active tokamaks, in the absence of intense neutron fluxes. In addition to the intended use of sapphire as protective windows for metal mirrors, existing tokamaks widely use sapphire vacuum windows for thermographic control of the first wall and divertor plates (Globus M2 [32], Tore-Supra [33], JT-60SA [34]), when introducing powerful gyratron radiation [35]). These windows are located at relatively short distances and in the line of sight of the plasma. Vacuum sapphire windows are supposed to be used in ITER [36]. Therefore, the issues of plasma purification of sapphire windows remain relevant in experiments on tokamaks.

Conclusion

After a twelve-hour exposure in an RF discharge in a mixture of 77 % H_2–23 % Ne and removal of a layer of material with a thickness of 270 nm, the surface roughness R_q decreased from 5.4 to 3.4 nm.

In the topographic image of the surface, local areas (sections) with reduced roughness ($R_q = 1$–2 nm) with alternating protrusions and depressions with a height and depth of up to 10 nm appeared between the remaining deep

grooves. Perhaps these regions are the nascent elements of a stationary structure fully formed at large thicknesses of the removed surface layer.

The stoichiometric composition of both the uppermost nanometer and deeper micron layers has not changed. Selective atomization of oxygen in an oxide with a relatively light cation Al^{3+} in a reducing medium with hydrogen atoms and ions was not observed. Under the influence of plasma, a polishing effect appeared on the original grooved surface. The transmission of light in the wavelength range of 400−1000 nm remained unchanged.

After applying an 80 nm thick aluminum film to the formed surface, it was removed in an RF discharge by peeling and physical spraying. Complete removal of Al during 1 h was accompanied by the removal of a sapphire layer with a thickness of 20−30 nm. The newly formed surface relief, after removal of the primary grooves, represented a cellular structure of pits with a depth of 5−10 nm relative to the surrounding protrusions with a height of 3−5 nm. The reduced light transmission ($< 1\%$) after deposition of the Al film was completely restored to its original value as a result of subsequent purification in an RF discharge.

Triple deposition of an Al film with a thickness of 30−40 nm onto the initial mechanically polished surface and triple cleaning in an RF discharge for 1 h in each cycle was accompanied by the removal of a layer of sapphire with a thickness of 10−15 nm. In these cleaning cycles, the aluminum film was removed first by peeling off individual sections with an area of $1-3\,\mu$m, and then by physical spraying. The removal of sections of the metal film by peeling was one of the reasons for the development of the cellular structure of the surface. After each cleaning cycle, the light transmission coefficient returned to the initial values. The final TC after three times cleaning turned out to be 1% higher than the initial values in the entire wavelength range.

The stability of light transmission of plates r-Al_2O_3 demonstrated in the study after exposure to RF discharge in a mixture of $77\%\,H_2-23\%$ Ne allows considering the studied metal precipitation removal technique promising for use in restoring the light transmission of protective windows in front of the first mirror in the divertor Thomson scattering diagnostics and vacuum windows of various optical diagnostics in the ITER tokamak under construction.

Acknowledgments

X-ray diffraction analysis, surface analysis using XPS, AFM examination of the surface of samples, and measurement of sapphire light transmission on a spectrophotometer were performed on the equipment of the Center for the Collective use of Physical Methods of Research ..of the Institute of Physical Chemistry and Electrochemistry of RAS.

Funding

The work was performed within the state assignment of the Ministry of Science and Higher Education of the Russian Federation No. 1023033100314-3-1.4.3.

Problem statement and formulation of technical requirements for the sapphire window of the scattered radiation of TS diagnostic system (sec. Introduction and task statement) were carried out with the support of the Ministry of Science and Higher Education of the Russian Federation within the framework of state assignment 124031800036-2.

Conflict of interest

The authors declare that they have no conflict of interest.

References

[1] E.E. Mukhin, V.V. Semenov, A.G. Razdobarin, S.Yu. Tolstyakov, M.M. Kochergin, G.S. Kurskiev, K.A. Podushnikova, S.V. Masyukevich, D.A. Kirilenko, A.A. Sitnikova, P.V. Chernakov, A.E. Gorodetsky, V.L. Bukhovets, R.Kh. Zalavutdinov, A.P. Zakharov, I.I. Arkhipov, Yu.P. Khimich, D.B. Nikitin, V.N. Gorshkov, A.S. Smirnov, T.V. Chernoizumskaja, E.M. Khilkevitch, S.V. Bulovich, V.S. Voitsenya, V.N. Bondarenko, V.G. Konovalov, I.V. Ryzhkov, O.M. Nekhaieva, O.A. Skorik, K.Yu. Vukolov, V.I. Khripunov, P. Andrew. Nucl. Fusion, **52**, 013017 (2012). DOI: 10.1088/0029-5515/52/1/013017

[2] E.E. Mukhin, G.S. Kurskiev, A.V. Gorbunov, D.S. Samsonov, S.Yu. Tolstyakov, A.G. Razdobarin, N.A. Babinov, A.N. Bazhenov, I.M. Bukreev, A.M. Dmitriev, D.I. Elets, A.N. Koval, A.E. Litvinov, S.V. Masyukevich, V.A. Senitchenkov, V.A. Solovei, I.B. Tereschenko, L.A. Varshavchik, A.S. Kukushkin, I.A. Khodunov, M.G. Levashova, V.S. Lisitsa, K.Yu. Vukolov, E.B. Berik, P.V. Chernakov, Al.P. Chernakov, An.P. Chernakov, P.A. Zatilkin, N.S. Zhiltsov, D.D. Krivoruchko, A.V. Skrylev, A.N. Mokeev, P. Andrew, M. Kempenaars, G. Vayakis, M.J. Walsh. Nucl. Fusion, **59** (8), 086052 (2019). DOI: 10.1088/1741-4326/ab/cd5

[3] A. Litnovsky, V.S. Voitsenya, R. Reichle, M. Walsh, A.G. Razdobarin, A. Dmitriev, N.A. Babinov, L. Marot, L. Moser, R. Yan, M. Rube, S. Moon, S.G. Oh, P. Shigin, A. Krimmer, V. Kotov, P. Mertens. Nucl. Fusion, **59** (6), 066029 (2019). DOI: 10.1088/1741-4326/ab1446 FIP/1-4

[4] D. Samsonov, I. Tereschenko, E. Mukhin, A. Gubal, Yu. Kapustin, V. Filimonov, N. Babinov, A. Dmitriev, A. Nikolaev, I. Komarevtsev, A. Koval, A. Litvinov, G. Marchii, A. Razdobarin, L. Snigirev, S. Tolstyakov, G. Marinin, D. Terentev, A. Gorodetsky, R. Zalavutdinov, A. Markin, V. Bukhovets, I. Arkhipushkin, A. Borisov, V. Khripunov, V. Mikhailovskii, V. Modestov, I. Kirienko, I. Buslakov, P. Chernakov, A. Mokeev, M. Kempenaars, P. Shigin. E. Drapiko. Nucl. Fusion, **62** (6), 086014 (2022). DOI: 10.1088/1741?4326/ac544d

[5] S. Moon, P. Peterson, M. Rubel, E. Fortuna-Zalesna, A. Widdowson, Jachmich, A. Litnovsky, E. Alves, JET Contributors. Nucl. Mater. Energy, **19**, 59 (2019). DOI: 10.1016/j.nme.2019.02.009

[6] A. Bortolon, R. Maingi, A. Nagy, J. Ren, J.D. Duran, A. Maan, D.C. Donovan, J.A. Boedo, D.L. Rudakov, A.W. Hyatt, T.W. Wilks, M.W. Shafer, C.M. Samuell, M.E. Fenstermacher, E.P. Gilson, R. Lunsford, D.K. Mansfield, T. Abrams, R. Nazikian and the DIII-D team. Nucl. Fusion, **60** (12), 126010 (2020). DOI: 10.1088/1741-4326/abaf31
[7] W. Xu, Z. Sun, R. Maingi, G.Z. Zuo, Y.W. Yu, C.L. Li, Y.H. Guan, Z.T. Zhou, X.C. Meng, M. Huang, L. Zhang, W. Gao, J.S. Hu. Nucl. Mater. Energy, **34** (3), 101359 (2023). DOI: 10.1016/j.nme.2022.101359
[8] A.M. Dmitriev, A.G. Razdobarin, L.A. Snigirev, D.I. Elets, I.M. Bukreev, N.A. Babinov, L.A. Varshavchik, E.E. Mukhin, D.S. Samsonov, S.Yu. Tolstyakov, An.P. Chernakov, D.V. Kovalenko, V.L. Pogkovyrov, A.D. Yaroshevskaya, V.A. Barsuk, I.B. Kupriyanov, V.L. Bukhovets, A.E. Gorodetsky, A.V. Markin, R.Kh. Zalavutdinov, I.A. Arkhipushkin, S.A. Krat, V.I. Polskij, A.F. Gurbich. Nucl. Mater. Energy, **30**, 101111 (2022). DOI: 10.1016/j.nme.2021.101111
[9] F. Leipold, R. Reichle, C. Vorppahl, E.E. Mukhin, A.M. Dmitriev, A.G. Razdobarin, D.S. Samsonov, L. Marot, L. Moser, R. Steiner, E. Meyer. Rev. Sci. Instrum., **87** (11), 11D439 (2016). DOI: 10.1063/1.4962055
[10] V.L. Bukhovets, A.E. Gorodetsky, R.Kh. Zalavutdinov, A.V. Markin, L.P. Kazansky, I.A. Arkhipushkin, A.P. Zakharov, A.M. Dmitriev, A.G. Razdobarin, E.E. Mukhin. Nucl. Mater. Energy, **12**, 458 (2017). DOI: 10.1016/j.nme.2017.05.002
[11] E.R. Dobrovinskaya, L.A. Litvynov, V. Pishchik. *Sapphire. Material, Manufacturing, Applications* (Springer Science + Business Media, LLC 2009), DOI: 10.1007/978-0-387-85695-7
[12] L.A. Litvynov. Ch. 13. *Aluminum Oxide*. In *Single Crystal of Electronic Materials* (Elsevier, 2019), p. 447–485. DOI: 10.1016/B978-0-08-102029-8.00013
[13] V.F. Tkachenko, O.A. Lukienenko, A.T. Budnikov, E.A. Vovk, S.I. Krivonogov, A.Ya. Dan'ko. Functional Materials, **18** (2), 171 (2011).
[14] A. Kallenbach, M. Bernert, R. Dux, L. Casali, T. Eich, L. Giannone, A. Herrmann, R. McDermott, A. Mlynek, H.W. Müller, F. Reimold, J. Schweinzer, M. Sertoli, G. Tardini, W. Treutterer, E. Viezzer, R. Wenninger, M. Wischmeier. ASDEX Upgrade Team. Plasma Phys. Control. Fusion, **55**, 124041 (2013). DOI: 10.1088/0741-3335/55/12/1240412
[15] M. Marin, J. Citrin, C. Giroud, C. Bourdelle, Y. Camenen, L. Garzotti, A. Ho, M. Sertoli JET Contributors. Nucl. Fusion, **63**, 016019 (2023). DOI: 10.1088/1741-4326/aca469
[16] S.S. Dovganyuk, L.B. Begrambekov, Yu.I. Rukina, E.A. Narskikh. Mater. XXVIII Mezhdunar. konf. „Vzaimodejstvie plazmy s poverhnost'yu", Sb. nauch. tr. (NIYAU MIFI, M., 2025), p. 76 (in Russian).
[17] A.E. Gorodetsky, L.A. Snigirev, A.V. Markin, V.L. Bukhovets, T.V. Rybkina, R.Kh. ZalavutdinovA.G. Razdobarin, E.E. Mukhin, A.M. Dmitriev, Tech. Phys., **67** (10), 1373 (2022). DOI: 10.21883/TF.2022.10.54365.108-22
[18] T. Nakamura, H. Matsuhashi, Y. Nagatomo. OKI Tecn. Rev., **71** (4), 200, 66 (2004).
[19] A.E. Gorodetsky, A.V. Markin, V.L. Bukhovets, T.V. Rybkina, R.Kh. Zalavutdinov, A.P. Zakharov, A.G. Razdobarin, E.E. Mukhin, A.M. Dmitriev. Tech. Phys. Lett., **50** (11), 12 (2024).
[20] E. Centurioni. Appl. Opt., **44** (35), 7532 (2005). DOI: 10.1364/AO.44.007532
[21] I.H. Malitson. J. Opt. Society America, **52** (12), 1377 (1962). DOI: 10.13641/jOSA.52.001377
[22] I.H. Malitson, M.J. Dodge. J. Opt. Society America, **62**, 1405 (1972).
[23] R. Cuerno, J.S. Kim. J. Appl. Phys., **128**, 180902 (2020). DOI: 10.1063/5.0021308
[24] Q. Bi, Z. Chen, Y. Liu, L. Tang, Y. Xi, W.Liu. Coatings, **10**, 949 (2020). DOI: 10.3390/coatings10100949
[25] B. Kahng, H. Jeong, A.-L. Barabasi. Appl. Phys. Lett., **78** (6), 805 (2001). DOI: 10.1063/1.1343468
[26] Electronic resource. SRIM-2008. *The stopping and range of ions in materials*. Available at: http://www.SRIM.org/
[27] K.C. Sabat, P. Rajput, R.K. Paramguru, B. Bhoi, B.K. Mishra. Plasma Chem. Plasma Process, **34**, 1 (2013). DOI: 10.1007/s11090-013-9484-2
[28] D.D. Wagman, W.H. Evans, V.B. Parker, R.H. Schumm, I. Halow, S.M. Bailey, K.L. Churney, R.L. Nutall. J. Phys. Chem. Reference Data, **11**, Supplement 2, 407 (1982).
[29] W. Eckstein. *Computer Simulation of Ion-Solid Interactions* (Springer-Verlag, Berlin, Heidelberg, 1991)
[30] M.I. Patino, R.P. Dorner, G.R. Tynan. Nucl. Mater. Energy, **23**, 100753 (2020). DOI: 10.1016/j.nme.2020.100753
[31] A.E. Gorodetsky, A.V. Markin, V.L. Bukhovets, V.I. Zolotarevsky, R.Kh. Zalavutdinov, E.E. Mukhin, A.G. Razdobarin. J. Surf. Investigation: X-ray, Synchrotron and Neutron Techniques, **15** (4), 660 (2021).
[32] V.A. Tokarev, V.K. Gusev, N.A. Khromov, A.V. Voronin, Yu.V. Petrov, N.V. Sakharov, A.N. Novokhatsky, V.B. Minaev, V.I. Varfolomeev, I.M. Balachenkov, A.Yu. Telnova, P.B. Shchegolev, N.N. Bakharev, G.S. Kurskiev, E.O. Kiselev, M.I. Patrov, E.A. Tyukhmeneva, S.Yu. Tolstyakov. *48 Mezhdunarodnaya (Zvenigorodskaya) konferenciya po fizike plazmy i UTS* (15–19 marta 2021, Zvenigorod), DOI: 10.34854/ICPAF.2021.48.1.039 (in Russian)
[33] G. Guilhem, J.L. Bondil, B. Bertrand, C. Desgrangers, M. Lipa, P. Messina, M. Missirlian, C. Portfaix, Reichle, H. Roche, A. Saille. Fusion Eng. Design, **74** (1–4), 879 (2005). DOI: 10.1016/j.fusengdes.2005.08.021
[34] T. Szepeci, S. Devis, N. Hajnal, K. Kamaiya, G. Kocsis, Á. Kovácsik, N. Oyama, C. Sozzi, S. Zoletnik. Fusion Eng. Design, **153**, 111505 (2020). DOI: 10.1016/j.fusengdes:2020.111505
[35] R. Magne, C. Darbos, S. Alberti, A. Barbuti, F. Bianchard, P. Cara. *International Vacuum Electronics Conference* (Monterey. CA. USA, 2000), DOI: 10.1109/OVE:EC.2000.847558
[36] V.S. Udintsev, P. Maquet, N. Gimbert, T. Giacomin, J. Guirao, S. Iglesias, Ch. Vacas, M.J. Walsh, S. Pak, B. Conway, M. Dopena, J.-M. Drevon, G. Eaton, S. Hughes, T. Darby, R. Bamber. IEEE Transactions on Plasma Science, **47** (1), 864 (2019). DOI: 10.1109/TPS.2018.28979407

Translated by A.Akhtyamov